Physiological and anatomical investigation of the auditory brainstem in the Fat-tailed dunnart (*Sminthopsis crassicaudata*)

Andrew Garrett [Corresp., 1, 2], Virginia Lannigan [2, 3], Nathanael Yates [3, 4], Jennifer Rodger [2, 3], Wilhelmina Mulders [3, 5]

1 Department of Systems Neuroscience, JFB Institute of Zoology and Anthropology, Bernstein Focus Neurotechnology (BFNT), Georg-August Universität Göttingen, Göttingen, Niedersachsen, Germany

2 School of Biological Sciences, University of Western Australia, Crawley, Western Australia, Australia

3 School of Human Sciences, M311, University of Western Australia, Crawley, Western Australia, Australia

4 The Queensland Brain Institute, QBI Building 79, University of Queensland, St Lucia, Queensland, Australia

5 Ear Science Institute Australia, Subiaco, Western Australia, Australia

Corresponding Author: Andrew Garrett
Email address: andrew-richard.garrett@biologie.uni-goettingen.de

The fat-tailed dunnart (*Sminthopsis crassicaudata*) is a small (10-20g) native marsupial endemic to the south west of Western Australia. Currently little is known about the auditory capabilities of the dunnart, and of marsupials in general. Consequently, this study sought to investigate several electrophysiological and anatomical properties of the dunnart auditory system. Auditory brainstem responses (ABR) were recorded to brief (5ms) tone pips at a range of frequencies (4-47.5 kHz) and intensities to determine auditory brainstem thresholds. The dunnart ABR displayed multiple distinct peaks at all test frequencies, similar to other mammalian species. ABR showed the dunnart is most sensitive to higher frequencies increasing up to 47.5 kHz. Morphological observations (Nissl stain) revealed that the auditory structures thought to contribute to the first peaks of the ABR were all distinguishable in the dunnart. Structures identified include the dorsal and ventral subdivisions of the cochlear nucleus, including a cochlear nerve root nucleus as well as several distinct nuclei in the superior olivary complex, such as the medial nucleus of the trapezoid body, lateral superior olive and medial superior olive. This study is the first to show functional and anatomical aspects of the lower part of the auditory system in the Fat-tailed dunnart.

1 Physiological and anatomical investigation of the auditory brainstem in the Fat-

2 tailed dunnart (*Sminthopsis crassicaudata*)

4 A. Garrett[3,4*], V. Lannigan[1,3], N. Yates[1,5], J. Rodger[1,3#], W.H.A.M. Mulders[1,2#]

6 [1] School of Human Sciences, M311, University of Western Australia, 35 Stirling Highway,

7 Crawley, Western Australia, 6009, Australia.

8 [2] Ear Science Institute Australia, 1/1 Salvado Rd, Subiaco, Western Australia, 6008, Australia.

9 [3] School of Biological Sciences, University of Western Australia, 35 Stirling Highway, Crawley,

10 Western Australia, 6009, Australia.

11 [4] Department of Systems Neuroscience, JFB Institute of Zoology and Anthropology, Bernstein

12 Focus Neurotechnology (BFNT), Georg-August-Universität Göttingen, Von-Siebold Strasse 6,

13 D-37075 Göttingen, Germany

14 [5] The Queensland Brain Institute, University of Queensland, St Lucia, Queensland, 4072,

15 Australia

17 # These authors have made equal contributions to this paper

19 * Correspondence: Andrew Garrett. Department of Systems Neuroscience, JFB Institute of

20 Zoology and Anthropology, Bernstein Focus Neurotechnology (BFNT), Georg-August-

21 Universität Göttingen, Von-Siebold Strasse 6, D-37075 Göttingen, Germany, email: andrew-

22 richard.garrett@biologie.uni-goettingen.de

24 Author declaration: The authors declare no conflicts of interest related to this manuscript.

25   Abstract

26   The fat-tailed dunnart (*Sminthopsis crassicaudata*) is a small (10-20g) native marsupial endemic

27   to the south west of Western Australia. Currently little is known about the auditory capabilities

28   of the dunnart, and of marsupials in general. Consequently, this study sought to investigate

29   several electrophysiological and anatomical properties of the dunnart auditory system. Auditory

30   brainstem responses (ABR) were recorded to brief (5ms) tone pips at a range of frequencies (4-

31   47.5 kHz) and intensities to determine auditory brainstem thresholds. The dunnart ABR

32   displayed multiple distinct peaks at all test frequencies, similar to other mammalian species.

33   ABR showed the dunnart is most sensitive to higher frequencies increasing up to 47.5 kHz.

34   Morphological observations (Nissl stain) revealed that the auditory structures thought to

35   contribute to the first peaks of the ABR were all distinguishable in the dunnart. Structures

36   identified include the dorsal and ventral subdivisions of the cochlear nucleus, including a

37   cochlear nerve root nucleus as well as several distinct nuclei in the superior olivary complex,

38   such as the medial nucleus of the trapezoid body, lateral superior olive and medial superior

39   olive. This study is the first to show functional and anatomical aspects of the lower part of the

40   auditory system in the Fat-tailed dunnart.

41

42

43

44

45

46

47

48

49

50

51 **Introduction**

52 Marsupials evolved separately from eutherian mammals in the Cretaceous period and now form

53 a highly diverse group with populations in the Americas and Australia (Luo, Yuan, Meng, & Ji,

54 2011; Nilsson et al., 2010). One marsupial, the fat-tailed dunnart (*Sminthopsis crassicaudata*), is

55 a small (10-20g) insectivorous Australian marsupial (Frey, 1991; Morton, 1978a) that is named

56 after its characteristic swollen tail that contains stored fat (Godfrey, 1968). The fat-tailed dunnart

57 is a solitary animal with a widespread distribution across the southern and western parts of

58 Australia inhabiting a variety of arid environments including open woodland, low scrublands,

59 grasslands on clay or sand soils and farmlands (Morton, 1978a). Within these varied

60 environments, the nocturnal dunnart hunts predominantly insects while itself being preyed upon

61 by other predators such as snakes, feral cats and barn owls (Morton, 1978b)

62 Interestingly, the visual system in the fat-tailed dunnart has been shown to be different from most

63 other marsupials as well as most eutherian mammals as they are trichromatic (Cowing, Arrese,

64 Davies, Beazley, & Hunt, 2008; Ebeling, Natoli, & Hemmi, 2010). Being predominantly

65 nocturnal (Levy, Dayan, Porter, & Kronfeld-Schor, 2019) the fat-tailed dunnart is likely to also

66 heavily depend on its sense of hearing and its ability to localise sound as a means for prey

67 detection, predator avoidance and species-specific communication (Osugi, Foster, Temple, &

68 Poling, 2011). Previous work in a range of marsupial families such as northern quoll (*Dasyurus*

69 *hallucatus)* (Aitkin, Nelson, & Shepherd, 1996), brush-tailed possums (*Trichosurus vulpecula*)

70 (Signal, Foster, & Temple, 2001), and the tammar wallaby (*Macropus eugenii*) (Liu, 2003; Liu,

71 Hill, & Mark, 2001) has shown that the overall structure of the auditory brainstem is largely

72 consistent within eutherian mammals, enabling the distinction of several subnuclei in cochlear

73 nuclei (CN), superior olivary complex (SOC) and inferior colliculus (Aitkin, 1998).

74 However, the relative size and detailed structure of the subcortical structures in the auditory

75 system is known to be highly varied both in eutherian mammals and marsupials (Glendenning &

76 Masterton, 1998). For example, the CN represents about 13% of the whole auditory system in the

77 swamp wallaby, but approximately 37% in the pocket gopher. In addition, there exists a large

78 degree of heterogeneity in the anatomical architecture of the CN and principal nuclei of the SOC

79 (Glendenning & Masterton, 1998). For example, in some of the Muridae such as rat, mouse and

80 gerbil (López, Merchán, Bajo, & Saldaña, 1993) as well as in some marsupials (Willard, 1993)

81   the auditory nerve contains a small group of large neurons, the so-called cochlear nerve root

82   neurons, whereas this does not appear to be the case in for instance cat or guinea pig. In the SOC,

83   the lateral superior olive (LSO) forms a S-shaped segment in many species such as guinea pig,

84   cat and gerbil (Grothe & Park, 2000) but has been described as a triangle shape in marsupials

85   (Aitkin 1996). In marsupials the cochlear nucleus is located medial to the restiform body,

86   whereas in other mammals the it is found lateral to the restiform body (Aitkin, 1996).

87   With regard to functional studies, the auditory brainstem response (ABR) has been shown to

88   reveal the typical waveforms (i.e. waves I-V present) between 1-90kHz with lowest thresholds

89   between 12-16kHz in the short-tailed opossum (*Monodelphus domestica*) (Reimer, 1996b).

90   Click-evoked ABRs obtained from tammar wallaby also showed typical peaks and the

91   appearance of the peaks during development correlated with the development of the known

92   anatomical substrates of the ABR waves (Liu, 2003; Liu, Hill, & Mark, 2001).

93   With the exception of a few references to the striped-faced dunnart (*Sminthopsis macroura*) by

94   Aitkin (1998) very little is known about the anatomy and physiology of the dunnart auditory

95   system. In view of the fact that the fat-tailed dunnart has specific adaptations in its visual system,

96   this paper explored functional and anatomical aspects of its auditory system to investigate

97   whether this sensory system also has distinct features compared to other marsupials. For this

98   purpose, we combined electrophysiological (ABR) and anatomical (Nissl staining) investigations

99   of the auditory brainstem in the dunnart. For the latter we focussed on cochlear nucleus and the

100   main nuclei in the SOC, known to be involved in sound localization.

101

Materials and Methods

103   *Animals*

104   Eight fat-tailed dunnarts (*Sminthopsis crassicaudata*) aged between 12 and 18 months (12-18g

105   weight) of either sex were used for this study. Precise age was not known but was estimated

106   based on arrival in the animal facilities, weight and time of experimentation. The animals were

107   separately housed in enriched cages containing running discs, rocks and a covered nest. Food

108   (Science Diet Sensitive Stomach Cat Food supplemented with live crickets and mealworms) and

109   water were supplied ad libitum. The vivariums were maintained at 22°C with a 12-hour Day

110   night cycle. All procedures conformed to NIH guidelines on the use of animals for

111   experimentation (USA) and were approved by the University of Western Australia's Animal

112   Ethic Committee (RA/3/100/1123).

113

114   *Auditory Brainstem Response Measurements*

115   The fat-tailed dunnarts were anaesthetised via intraperitoneal injection with ketamine (75mg/kg)

116   and medetomidine (1mg/kg). Animals were maintained at near physiological temperature (38°C)

117   using both a heating pad and an ambient room heater for the entirety of the auditory brainstem

118   response (ABR) recording (60-90 minutes per animal). ABRs were measured as previously

119   described (Yates, Robertson, Martin-Iverson, & Rodger, 2014). In brief, ABRs were recorded in

120   a sound attenuated room and sound stimuli were generated by custom made Neurosound

121   software (M. Lloyd Cambridge) via a RME DIGI 9636 sound card (96 kHz sampling rate).

122   Average ABRs (n=400 stimuli) were evoked using pure tone bursts (5ms duration, 1ms rise-fall-

123   time, rate 10/s), delivered to the animal using a plastic cone attached to a reverse driven ¼ inch

124   condenser microphone (Brüel and Kjær type 4134). The sound-output was calibrated at the level

125   of the eardrum using a Brüel & Kjær pistonphone (94dB SPL at 1000Hz) (Yates et al., 2014).

126   The acoustic coupler was placed using a surgical microscope to touch the lower edge of the left

127   tragus and was directed towards external auditory meatus. During the course of the experiments,

128   we observed no movement of the animal or auditory coupler.

129   ABR responses were recorded via an insulated silver-wire electrode inserted subdermally at the

130   vertex. A reference electrode was placed above the left mastoid at the base of the pinna and a

131   ground electrode was inserted into the tail. Differential recordings were made using an AC

132   coupled amplifier (DAM50, World Precision Instruments) with a gain of 1000x and band pass

133   filtering at (300-3000Hz). Average ABR responses were sampled by Powerlab/4ST (AD

134   Instruments) and stored for offline analyses.

135   ABR thresholds were determined at 4, 8, 16, 24, 32 and 47.5 kHz. In view of the sampling rate

136   of our sound card 47.5 kHz was the maximum frequency tested. Each sound stimulus was

137   presented first at 10dB attenuation followed by sound intensities decreasing in 10dB increments

138 until after the disappearance of overt ABR peaks (I and V) in the recording. Upon disappearance

139 of the ABR, the sound intensity was increased in 5dB steps until the visual reappearance of the

140 peaks in the waveform. Sound stimuli were converted into sound pressure (SPL, re 20μPa) levels

141 using a Bruel and Kjaer pistonphone (94dB SPL at 1000Hz). ABR traces were analyzed using

142 AxoGraph X V1.5.0 (J. Clements, Australia) and thresholds were determined by visual

143 inspection. ABR threshold was estimated as the lowest intensity where peaks I and V could still

144 be identified. The threshold estimation procedure employed here, was undertaken by 3 different

145 observers and yielded consistent estimates (less than 5 dB difference).

146

147 *Histological preparation*

148 Dunnarts were terminally anaesthetised with 0.2ml euthal (pentobarbitone sodium 170mg/mL,

149 phenytoin sodium 25mg/mL). Animals were then perfused with saline (0.9%) followed by

150 paraformaldehyde (4% in 0.1M phosphate buffered saline, PBS). Regions of brainstem

151 containing auditory nuclei were removed and cryoprotected (30% sucrose in 0.1M PBS for 24h)

152 and sectioned at 30μm using a cryostat (Leica CM1900).

153 For cresyl violet staining, horizontal sections were washed with PBS for four minutes and then

154 dehydrated in graded ethanol solutions (70% - 95%, one minute). Slides were heated in a

155 microwave for 2 minutes in a 500mL solution of 95% ethanol and 5% glacial acetic acid

156 (Sigma), followed by rehydration in descending ethanol solutions (95% to 70%, 20 seconds

157 each) and washed in PBS for one minute. Sections were then placed in warmed cresyl violet

158 solution (0.5% cresyl violet) for eight minutes. After staining, sections were rapidly exchanged

159 through ascending ethanol solutions (70%-95%, 15 seconds each) and differentiated at room

160 temperature in 95% ethanol and 5% acetic acid for 5 minutes. Finally, slides were washed with

161 three 100% ethanol and cleared in xylene. Slides were cover-slipped with DePeX (ProSciTech)

162 mounting media and dried overnight prior to microscopy.

163

164

165

166 *Microscopy and analysis*

167 Images of cresyl violet stained sections were captured using an Olympus DP70 camera and DP

168 Controller (Olympus Corporation, image size 4080x3072pixels). High-power micrographs were

169 captured using a Nikon DS-U2/L2 camera with NIS-Elements (Nikon AR 3.0, image size

170 2560x1920pixels). Using standard anatomical markers such as neuronal shape, neuronal density,

171 and somatic alignment, the auditory nuclei (CN and SOC) were identified in the dunnart. Nuclei

172 were observed under low power to determine the area and extent of the nucleus. Images for

173 publication underwent minor adjustments in brightness and contrast.

174

175 **Results**

176 *Auditory Brainstem Response*

177 A typical ABR was observed in the fat-tailed dunnart (figure 1). At moderate to high sound

178 intensities, the ABR showed five distinct peaks within the first 6ms after onset of the tone

179 stimuli. ABRs were evoked at all frequencies tested in this study (between 4 and 47.5 kHz).

180 ABR threshold was estimated as the lowest intensity where peak I and V could still be identified

181 (typical example at 47.5kHz shown in figure 2a). Average thresholds (n= 6-8) depicted as

182 audiograms (figure 2b) reveal the fat-tailed dunnart ABR is more sensitive (lower thresholds)

183 with increasing frequency. Currently however, it cannot be established whether 47.5 kHz is the

184 most sensitive frequency or if ABR thresholds decline rapidly at higher frequencies.

185 In agreement with the known characteristics of ABR responses, peak I amplitudes increased with

186 increasing sound intensity (figure 2c). Similarly, increasing sound intensities resulted in a

187 shortening of ABR latencies (data for 4, 24 and 47.5kHz shown in figure 2d).

188

189 *Histological analysis*

190 *The cochlear nerve root and cochlear nuclei*

191 Similar to other known marsupial species such as the brush-tailed possum and quoll, the cochlear

192 nuclei (CN) reside medial to the restiform body (rb in figure 3a-c). The ventral cochlear nucleus

193 (VCN) as a whole is clearly identifiable in the dunnart (figure 3c,h) with round small closely

194 packed cells of the anteroventral cochlear nucleus (AVCN) in rostral levels to the dorsal cochlear

195 nucleus (DCN). A sparsely populated posteroventral cochlear nucleus (PVCN) containing large

196 nuclei was observed in more caudal sections containing the other cochlear nuclei (figure

197 3c,d,e,f).

198 On gross appearance, the dunnart DCN is a trigonal shaped nucleus. In more caudal sections, a

199 prominent tri-laminar DCN could clearly be subdivided into a molecular (I in figure 3f), fusiform

200 layer (II in figure 3f) and polymorphic layers (III in figure 3f). The DCN was bounded laterally

201 by the small cell cap layer (scc, figure 3d, f).

202 Briefly. the dunnart also shows a clearly defined cochlear nerve root nucleus (CNR) (figure 3e

203 and g), consisting of large neurons clustered within the passing nerve fascicles.

204

205 *The superior olivary complex nuclei*

206 The nuclei of the superior olivary complex (SOC) in the dunnart closely resembled their

207 anatomical correlates found in eutherian mammals. Of the three principal SOC nuclei lateral

208 superior olive (LSO), medial superior olive (MSO), and the medial nucleus of the trapezoid body

209 (MNTB), the most prominent and distinguishable nucleus in the dunnart was the MNTB (figure

210 4a,b). The MNTB occupied a familiar position within the brainstem and the cells of the MNTB

211 were not densely packed presumably due to their location within the passing trapezoid body

212 projection (see figure 4 b). A small MSO (typically observed within one to two histological

213 sections) was observed as a linear cluster of pleiomorphic cells aligned along a dorsal-ventral

214 axis (figure 4a-c).

215 The lateral superior olive (LSO) of the dunnart was not as well defined as found in similarly

216 sized eutherian species (figure 4c). Despite this, the LSO was observed as a round nucleus

217 located near the latero-ventral surface of the brainstem in transverse sections often containing the

218 MNTB. The LSO could be subdivided into densely stained elongated cells in more marginal

219 areas (figure 4c, lso(m)), whereas lightly stained bipolar nuclei were found to occupy more core

220 or central locations (figure 4c, lso(c)).

221 A nucleus corresponding to superior paraolivary nucleus (SPN, figure 4 a-c), was observed

222 residing dorsomedially between the MNTB and the MSO. Somata in this region contained large

223 densely stained multipolar cells with no clear systematic orientation.

224

225

226 **Discussion**

227 Here we characterise some of the anatomical and electrophysiological features of the ascending

228 auditory pathway in the fat-tailed dunnart. With the exception of Aitkin (1998), there has been

229 very little characterisation of the dunnart auditory system, therefore we sought to establish

230 normative values of the fat-tailed dunnart auditory system. In addition to identifying common

231 auditory nuclei, we found that the anesthetised fat-tailed dunnart auditory system is remarkably

232 sensitive to high frequency stimuli.

233 The ABR represents the average response to repetitive sound stimuli of neuronal populations in

234 the auditory pathway. Waveform analysis of the ABR revealed 5 definite peaks (Reimer, 1996)

235 with short latency, corresponding to the action-potential volleys from the auditory nerve through

236 to inferior colliculus (Liu et al., 2001). In the current study, not only were we still able to evoke

237 ABR responses to high frequency stimuli (47.5kHz), but ABR thresholds improved at high

238 frequencies. These ABR findings are puzzling and present a contrast to the only previously

239 published data from a dunnart species (*Sminthopsis macroaura*), which displayed a frequency

240 range of 1-40kHz and a minimum, or best threshold at 10kHz (Aitkin, 1998). However, this

241 study was limited by low animal numbers (n=2) and lack of detail in the methodology, making it

242 unclear whether 40 kHz was the highest frequency attempted.

243 Nonetheless, high frequency sensitivity is quite common in small non-echolocating mammals

244 such as the leaf-eared mouse and spiny mouse (Heffner, Koay, & Heffner, 2001). In fact, upon

245 closer inspection of cochlear and ABR audiograms taken from several rodent species including

246 the mouse (*Mus musculus*), a second local minimum is present (20-30dB SPL) at around 50kHz

247 (Ehret, 1976; Heffner et al., 2001), and similarly, secondary local minima are also found in echo-

248 locating mammals (~15dB SPL at >45kHz) (Koay, Heffner, & Heffner, 1998).

249   With the exception of the cat (*Felis catus*), animals with smaller head sizes have small functional

250   interaural distances and tend to have higher audible frequencies (Heffner et al., 2001; Koay et al.,

251   1998). In agreement with this, another marsupial, the northern quoll (*Dasyurus hallucatus*)

252   which is larger than the dunnart (adults 400g, 5cm snout-ear), is most sensitive at 10kHz (10dB

253   SPL) with rapid loss of sensitivities at 40kHz (50-80dB SPL) (Aitkin, Nelson, & Shepherd,

254   1994; Oakwood, 2002). Similarly, the Brazilian short-tailed opossum (*Monodelphis domestica*)

255   also a marsupial larger than the fat-tailed dunnart (rat-size) shows best thresholds between 8 and

256   12 kHz (20 dB SPL) and an upper audible frequency limit of 60kHz (Reimer, 1995). Therefore,

257   given its small size (12-18g), the high frequency sensitivity observed in the fat-tailed dunnart

258   may be in line with its size, but conflicts with the limited data from the stripe faced dunnart

259   (Aitkin, 1998), which is of similar size. Therefore, we cannot exclude the possibility that this

260   audiogram of the fat-tailed dunnart represents a specific adaptation to its auditory environment,

261   in line with the specific adaptation found in its visual system (Cowing et al., 2008; Ebeling et al.,

262   2010). The reasons for such specialised adaptations within its sensory system remain unclear. As

263   discussed in Ebeling et al. it may represent specific adaptations to the visual and auditory

264   ecology or, alternatively, adaptations in early ancestors (Ebeling et al., 2010).

265   The anatomy of the auditory brainstem in the fat-tailed dunnart reveals a similar pattern of

266   auditory nuclei as reported previously across a range of marsupials (Aitkin, 1998). The CNR is

267   present in many small marsupials including the yellow-bellied glider (*Petaurus australis*),

268   Northern quoll (Aitkin, Byers, & Nelson, 1986) but also in muridae (López et al., 1993;

269   Merchan, Collia, Lopez, & Saldana, 1988) While neurons in the CNR nucleus are considered as

270   an extension of the ventral cochlear nucleus (Osen, Lopez, Slyngstad, Ottersen, & Storm-

271   Mathisen, 1991), it projects to motor components of the pontine reticular and facial nuclei

272   (Lopez, Saldana, Nodal, Merchan, & Warr, 1999). Although few in number, neurons in the CNR

273   nucleus in the rat respond to sound and thus likely represent an initial auditory nucleus (Sinex,

274   Lopez, & Warr, 2001). Given its early position within the auditory pathway, sensitivity to sound,

275   and efferent projections to the pontine motor nuclei, the CNR nucleus is thought to play a role in

276   sensorimotor control of acoustic startle responses (Lee, Lopez, Meloni, & Davis, 1996).

277   The auditory cochlear nuclei in the dunnart were similar in location to other marsupial species

278   studied such as the brush-tailed possum (*Trichosurus vulpecula*) (Aitkin & Kenyon, 1981),

279   multiple glider species (Aitkin, 1996), and northern quoll (Aitkin et al., 1986). Also in agreement

280   with other marsupials, the fat-tailed dunnart's trilaminar DCN was larger than the VCN (Aitkin,

281   1996, 1998). Despite widespread variation across mammalian species (Glendenning &

282   Masterton, 1998; Illing, Kraus, & Michler, 2000), the organisation of the SOC was again largely

283   consistent with previous reports. In common laboratory rodents, the three main SOC (LSO, MSO

284   and MNTB) as well as the SPN, are known targets of the cochlear nuclei and it is likely that a

285   similar connectivity exists in marsupials (Aitkin et al., 1986; Bazwinsky-Wutschke, Hartig,

286   Kretzschmar, & Rubsamen, 2016; Schofield, 1995). The presence of the MSO is not surprising

287   as it is known to persist in almost all mammalian species including the mouse (Fischl et al.,

288   2016; Ollo & Schwartz, 1979). Furthermore, the location and appearance of the MSO as a linear

289   nucleus in the dunnart is consistent with previous reports in arboreal marsupials (Aitkin, 1996).

290   The MSO is involved in detecting interaural timing differences related to sound localization of

291   lower frequencies (Grothe & Sanes, 1994). Therefore, it is likely that the functional role of the

292   MSO in these small animals with high frequency sensitivity is relatively limited (Grothe &

293   Pecka, 2014) and hence its small size in the fat-tailed dunnart is as expected. The LSO and

294   MNTB, involved in detection of higher frequencies based on interaural level differences (Caird

295   & Klinke, 1983; Grothe & Koch, 2011) were both present in the fat-tailed dunnart in line with its

296   high frequency sensitivity.

297   The relative size of the MNTB is known to vary between species, its relative size being about 5%

298   of the subcortical auditory system in kangaroo rat and less than 1% in humans (Glendenning &

299   Masterton, 1998). In addition, a study by Hilbig et al comparing different primates, showed a

300   marked reduction in MNTB size from macaque to human (Hilbig, Beil, Hilbig, Call, & Bidmon,

301   2009). The MNTB in the fat-tailed dunnart was clearly distinguishable with large neurons

302   comparable to the anatomy in rat (Reuss, Disque-Kaiser, De Liz, Ruffer, & Riemann, 1999).

303   Taken together, the presence of the large well defined MNTB, which is known to provide

304   powerful and precisely-timed glycinergic inhibition to the ipsilateral LSO, MSO and SPN

305   (Adams & Mugnaini, 1990; Sanes & Friauf, 2000), completes known anatomical circuits

306   involved with sound-localisation in many eutherian species (Kapfer, Seidl, Schweizer, & Grothe,

307   2002; Sanes & Friauf, 2000; Tollin, 2003).

308 The LSO is often described as an S-shaped or horseshoe shaped nucleus in many species such as

309 guinea pig, cat and gerbil (Grothe & Park, 2000). In contrast to the mouse (Ollo & Schwartz,

310 1979), a distinct shape could not be observed in our histological material. Rather the LSO

311 boundary in the dunnart remained diffuse, in line with the description of Aitkin (1996) in some

312 arboreal marsupials (Aitkin, 1996). Despite the lack of a clear boundary, the LSO did contain

313 subdivisions (marginal and core) which has been reported previously by Willard & Martin

314 (1983) in the opossum (Willard & Martin, 1983).

315 While the presence of CN and SOC in the dunnart suggests an ability to process incoming

316 auditory information particularly in terms of sound localisation, further investigations into the

317 synaptic morphology, neurochemistry and electrophysiology would further help to refine our

318 understanding of the roles these nuclei play within the dunnart and their environment.

319 **Conclusions**

320 Here we show that the fat-tailed dunnart is an animal species that displays a remarkable high

321 frequency sensitivity. In addition, the auditory brainstem nuclei reveal a large and well

322 developed CN as well as a MNTB. These nuclei are important in early binaural auditory

323 processing and sound localisation, and their presence in the dunnart suggests similar processing

324 capabilities. In addition to extending the ABR audiograms to higher frequencies, it would be of

325 immediate interest to determine how the hearing sensitivities correspond to species specific

326 communication as well as predator / prey detection and avoidance. (Aitkin et al., 1994). In light

327 of recent reports on the role of the DCN in the analysis of vocalisations (Roberts & Portfors,

328 2015), it would be of interest to determine if the DCN performs a similar role in the marsupial.

329

330

331

332

333

334

335   **References:**

336   Adams, J. C., & Mugnaini, E. (1990). Immunocytochemical evidence for inhibitory and disinhibitory
337   circuits in the superior olive. *Hear Res, 49*(1-3), 281-298.
338   Aitkin, L. (1996). The anatomy of the cochlear nuclei and superior olivary complex of arboreal Australian
339   marsupials. *Brain Behav Evol, 48*(2), 103-114. doi:10.1159/000113189
340   Aitkin, L. (1998). *Hearing, the brain, and auditory communication in marsupials* (Vol. 38). Berlin
341   Heidelberg: Springer-Verlag.
342   Aitkin, L., Byers, M., & Nelson, J. (1986). Brain stem auditory nuclei and their connections in a
343   carnivorous marsupial, the northern native cat (Dasyurus hallucatus). *Brain Behav Evol, 29*(1-2),
344   1-16.
345   Aitkin, L., & Kenyon, C. (1981). The auditory brain stem of a marsupial. *Brain Behav Evol, 19*(3-4), 126-
346   143.
347   Aitkin, L., Nelson, J., & Shepherd, R. (1994). Hearing, vocalization and the external ear of a marsupial, the
348   northern Quoll, Dasyurus hallucatus. *J Comp Neurol, 349*(3), 377-388.
349   doi:10.1002/cne.903490305
350   Bazwinsky-Wutschke, I., Hartig, W., Kretzschmar, R., & Rubsamen, R. (2016). Differential morphology of
351   the superior olivary complex of Meriones unguiculatus and Monodelphis domestica revealed by
352   calcium-binding proteins. *Brain Struct Funct, 221*(9), 4505-4523. doi:10.1007/s00429-015-1181-x
353   Caird, D., & Klinke, R. (1983). Processing of binaural stimuli by cat superior olivary complex neurons. *Exp
354   Brain Res, 52*(3), 385-399.
355   Cowing, J. A., Arrese, C. A., Davies, W. L., Beazley, L. D., & Hunt, D. M. (2008). Cone visual pigments in
356   two marsupial species: the fat-tailed dunnart (Sminthopsis crassicaudata) and the honey possum
357   (Tarsipes rostratus). *Proc Biol Sci, 275*(1642), 1491-1499. doi:10.1098/rspb.2008.0248
358   Ebeling, W., Natoli, R. C., & Hemmi, J. M. (2010). Diversity of color vision: not all Australian marsupials
359   are trichromatic. *PLoS One, 5*(12), e14231. doi:10.1371/journal.pone.0014231
360   Ehret, G. (1976). Development of absolute auditory thresholds in the house mouse (Mus musculus). *J
361   Am Audiol Soc, 1*(5), 179-184.
362   Fischl, M., Burger, R., Schmidt-Pauly, M., Alexandrova, O., Sinclair, J., Grothe, B., . . . Kopp-Scheinpflug, C.
363   (2016). Physiology and anatomy of neurons in the medial superior olive of the mouse. *J
364   Neurophysiol, 116*(6), 2676-2688. doi:10.1152/jn.00523.2016
365   Frey, H. (1991). Energetic Significance of Torpor and Other Energy-conserving Mechanisms in Free-living
366   Sminthopsis crassicaudata (Marsupialia : Dasyuridae) *Aust J Zool, 39*, 689-708.
367   Glendenning, K., & Masterton, R. (1998). Comparative morphometry of mammalian central auditory
368   systems: variation in nuclei and form of the ascending system. *Brain Behav Evol, 51*(2), 59-89.
369   Godfrey, G. (1968). Body-Temperature and Torpor in Sminthopsis Crassicaudata and S Larapinta
370   (Marsupialia-Dasyuridae). *Journal of Zoology, 156*, 499.
371   Grothe, B., & Koch, U. (2011). Dynamics of binaural processing in the mammalian sound localization
372   pathway--the role of GABA(B) receptors. *Hear Res, 279*(1-2), 43-50.
373   doi:10.1016/j.heares.2011.03.013
374   Grothe, B., & Park, T. J. (2000). Structure and function of the bat superior olivary complex. *Microsc Res
375   Tech, 51*(4), 382-402. doi:10.1002/1097-0029(20001115)51:4<382::AID-JEMT7>3.0.CO;2-7
376   Grothe, B., & Pecka, M. (2014). The natural history of sound localization in mammals--a story of
377   neuronal inhibition. *Front Neural Circuits, 8*, 116. doi:10.3389/fncir.2014.00116
378   Grothe, B., & Sanes, D. H. (1994). Synaptic inhibition influences the temporal coding properties of medial
379   superior olivary neurons: an in vitro study. *J Neurosci, 14*(3 Pt 2), 1701-1709.

380 Heffner, R., Koay, G., & Heffner, H. (2001). Audiograms of five species of rodents: implications for the
381   evolution of hearing and the perception of pitch. *Hear Res, 157*(1-2), 138-152.
382 Hilbig, H., Beil, B., Hilbig, H., Call, J., & Bidmon, H. J. (2009). Superior olivary complex organization and
383   cytoarchitecture may be correlated with function and catarrhine primate phylogeny. *Brain
384   Struct Funct, 213*(4-5), 489-497. doi:10.1007/s00429-008-0201-5
385 Illing, R., Kraus, K., & Michler, S. (2000). Plasticity of the superior olivary complex. *Microsc Res Tech,
386   51*(4), 364-381. doi:10.1002/1097-0029(20001115)51:4<364::AID-JEMT6>3.0.CO;2-E
387 Kapfer, C., Seidl, A. H., Schweizer, H., & Grothe, B. (2002). Experience-dependent refinement of
388   inhibitory inputs to auditory coincidence-detector neurons. *Nat Neurosci, 5*(3), 247-253.
389   doi:10.1038/nn810
390 Koay, G., Heffner, R., & Heffner, H. (1998). Hearing in a megachiropteran fruit bat (Rousettus
391   aegyptiacus). *J Comp Psychol, 112*(4), 371-382.
392 Lee, Y., Lopez, D., Meloni, E., & Davis, M. (1996). A primary acoustic startle pathway: obligatory role of
393   cochlear root neurons and the nucleus reticularis pontis caudalis. *J Neurosci, 16*(11), 3775-3789.
394 Levy, O., Dayan, T., Porter, W. P., & Kronfeld-Schor, N. (2019). Time and ecological resilience: can diurnal
395   animals compensate for climate change by shifting to nocturnal activity? *Ecological
396   Monographs, 89*(1), e01334.
397 Liu, G. (2003). Functional development of the auditory brainstem in the tammar wallaby (Macropus
398   eugenii): the superior olivary complex and its relationship with the auditory brainstem response
399   (ABR). *Hear Res, 175*(1-2), 152-164.
400 Liu, G., Hill, K., & Mark, R. (2001). Temporal relationship between the auditory brainstem response and
401   focal responses of auditory nerve root and cochlear nucleus during development in the tammar
402   wallaby (Macropus eugenii). *Audiol Neurootol, 6*(3), 140-153. doi:10.1159/000046821
403 López, D. E., Merchán, M. A., Bajo, V. M., & Saldaña, E. (1993). The Cochlear Root Neurons in the Rat,
404   Mouse and Gerbil. In M. A. Merchán, J. M. Juiz, D. A. Godfrey, & E. Mugnaini (Eds.), *The
405   Mammalian Cochlear Nuclei: Organization and Function* (pp. 291-301). Boston, MA: Springer US.
406 Lopez, D. E., Saldana, E., Nodal, F. R., Merchan, M. A., & Warr, W. B. (1999). Projections of cochlear root
407   neurons, sentinels of the rat auditory pathway. *J Comp Neurol, 415*(2), 160-174.
408 Luo, Z. X., Yuan, C. X., Meng, Q. J., & Ji, Q. (2011). A Jurassic eutherian mammal and divergence of
409   marsupials and placentals. *Nature, 476*(7361), 442-445. doi:10.1038/nature10291
410 Merchan, M. A., Collia, F., Lopez, D. E., & Saldana, E. (1988). Morphology of cochlear root neurons in the
411   rat. *J Neurocytol, 17*(5), 711-725.
412 Morton, S. R. (1978a). Ecological Study of Sminthopsis-Crassicaudata (Marsupialia Dasyurdae).1.
413   Distribution, Study Areas and Methods. *Australian Wildlife Research, 5*(2), 151-162.
414 Morton, S. R. (1978b). Ecological Study of Sminthopsis-Crassicaudata (Marsupialia Dasyuridae). 2.
415   Behavior and Social-Organization. *Australian Wildlife Research, 5*(2), 163-182.
416 Nilsson, M. A., Churakov, G., Sommer, M., Tran, N. V., Zemann, A., Brosius, J., & Schmitz, J. (2010).
417   Tracking marsupial evolution using archaic genomic retroposon insertions. *PLoS Biol, 8*(7),
418   e1000436. doi:10.1371/journal.pbio.1000436
419 Oakwood, M. (2002). Spatial and social organization of a carnivorous marsupial Dasyurus hallucatus
420   (Marsupialia: Dasyuridae). *J Zool Lond, 257*, 237-248.
421 Ollo, C., & Schwartz, I. R. (1979). The superior olivary complex in C57BL/6 mice. *Am J Anat, 155*(3), 349-
422   373. doi:10.1002/aja.1001550306
423 Osen, K. K., Lopez, D. E., Slyngstad, T. A., Ottersen, O. P., & Storm-Mathisen, J. (1991). GABA-like and
424   glycine-like immunoreactivities of the cochlear root nucleus in rat. *J Neurocytol, 20*(1), 17-25.
425 Osugi, M., Foster, T. M., Temple, W., & Poling, A. (2011). Behavior-based assessment of the auditory
426   abilities of brushtail possums. *J Exp Anal Behav, 96*(1), 123-138. doi:10.1901/jeab.2011.96-123

427 Reimer, K. (1995). Hearing in the marsupial Monodelphis domestica as determined by auditory-evoked
428   brainstem responses. *Audiology, 34*(6), 334-342.
429 Reimer, K. (1996). Characterization of the brainstem auditory evoked potential (BAEP) in the grey short-
430   tailed opossum (Monodelphis domestica). *Audiology, 35*(4), 204-216.
431 Reuss, S., Disque-Kaiser, U., De Liz, S., Ruffer, M., & Riemann, R. (1999). Immunfluorescence study of
432   neuropeptides in identified neurons of the rat auditory superior olivary complex. *Cell Tissue Res,*
433   *297*(1), 13-21.
434 Roberts, P. D., & Portfors, C. V. (2015). Responses to Social Vocalizations in the Dorsal Cochlear Nucleus
435   of Mice. *Front Syst Neurosci, 9*, 172. doi:10.3389/fnsys.2015.00172
436 Sanes, D. H., & Friauf, E. (2000). Development and influence of inhibition in the lateral superior olivary
437   nucleus. *Hear Res, 147*(1-2), 46-58.
438 Schofield, B. R. (1995). Projections from the cochlear nucleus to the superior paraolivary nucleus in
439   guinea pigs. *J Comp Neurol, 360*(1), 135-149. doi:10.1002/cne.903600110
440 Sinex, D. G., Lopez, D. E., & Warr, W. B. (2001). Electrophysiological responses of cochlear root neurons.
441   *Hear Res, 158*(1-2), 28-38.
442 Tollin, D. J. (2003). The lateral superior olive: a functional role in sound source localization.
443   *Neuroscientist, 9*(2), 127-143. doi:10.1177/1073858403252228
444 Willard, F. H. (1993). Postnatal Development of Auditory Nerve Projections to the Cochlear Nucleus in
445   Monodelphis Domestica. In M. A. Merchán, J. M. Juiz, D. A. Godfrey, & E. Mugnaini (Eds.), *The*
446   *Mammalian Cochlear Nuclei: Organization and Function* (pp. 29-42). Boston, MA: Springer US.
447 Willard, F. H., & Martin, G. F. (1983). The auditory brainstem nuclei and some of their projections to the
448   inferior colliculus in the North American opossum. *Neuroscience, 10*(4), 1203-1232.
449   doi:10.1016/0306-4522(83)90109-4
450 Yates, N., Robertson, D., Martin-Iverson, M., & Rodger, J. (2014). Auditory brainstem responses of
451   ephrin-A2, ephrin-A5(-/-) and ephrin-A2A5(-/-) mice. *Audiol Neurootol, 19*(2), 115-126.
452   doi:10.1159/000357029

453

454

455

456

457

458

459

460

461

462   **Figure legends**

463   **Figure 1.** Characteristic ABR recording from the fat-tailed dunnart (tone burst indicated with

464   black bar below the graph, 47.5 kHz, 5 ms duration, 52 dB SPL). Grey line represents the

465   background noise from the recording equipment. Main peaks of ABR indicated by roman

466   numerals and accompanied by abbreviated corresponding auditory nuclei. AN – auditory nerve,

467   CV- cochlear nuclei, SOC – superior olivary nuclei, LL – lateral lemniscus, IC- inferior

468   colliculus.

469

470   **Figure 2.** ABR thresholds in fat-tailed dunnart. (a): ABR recordings at 6 different intensities (42,

471   32, 22, 12, 7 and 2 dB SPL indicated right of waveforms) in response to a 47.5 kHz tone burst.

472   Waveform corresponding to ABR threshold (disappearance of peaks I and V – shown by

473   asterisks at top) is shown in thick black line. Black bar underneath waveforms indicates duration

474   of tone burst. (b): Audiogram showing ABR thresholds at different frequencies. Individual

475   animal thresholds are shown in grey with numbers in brackets above each point indicate number

476   of animals per data point. Due to several animals with the same thresholds, the number of

477   individual response points, may not appear to correspond with the number of animal in

478   parenthesis (c): Input-output function of the peak I amplitude at 4, 24 and 47.5 kHz. (d) Input-

479   output function of the latency of peak I at 4, 24 and 47.5 kHz. Each data point shows mean ±

480   SEM. N.B. in panel (c) and (d) some of the points at very low sound intensity are the values

481   derived from 1 or 2 animals.

482

483   **Figure 3**. Overview of the fat-tailed dunnart auditory brainstem. Nissl staining of transverse

484   sections reveals prominent auditory nerve root nucleus and cochlear nuclei. Images are organised

485   caudal to rostral. The dorsal cochlear nucleus resides medio-dorsal to the restiform body in the

486   caudal regions (shown in a, with high power image in b). (c and d): More rostrally the ventral

487   cochlear nucleus shows prominently as well. (d), (e), and (f): further rostral the trilaminar

488   arrangement of the dorsal cochlear nucleus is clearly visible (f) as well as the cochlear nerve root

489   nucleus (g). At more rostral level (h) the ventral cochlear nucleus shows a separation between

490   posteroventral and anteroventral cochlear nucleus. Scale bars are 500µm in a, c, e, h and 200µm

491   in b,d and f,g. Distance between panel a and c: 240µm, between c and e 90µm, and between e

492   and h 210µm. Section coordinates in panel (h) are for all sections. Abbreviations: cnr – cochlear

493   nerve root, cb – cerebellum, dcn – dorsal cochlear nucleus, fn – facial nucleus, rb – restiform

494   body, avcn – anteroventral cochlear nucleus, pvcn- posteroventral cochlear nucleus, in panel f: I

495   – molecular later II – fusiform layer III – polymorphic layer

496

497   **Figure 4**. Transverse sections of the superior olivary complex (SOC) nuclei in the fat-tailed

498   dunnart. The four main nuclei evident include the medial nucleus of the trapezoid body (MNTB)

499   (a and b) residing within the fibres of the trapezoid body (tb marked in a). The superior

500   paraolivary nucleus (SPN) is located dorsomedial to the MNTB. Located laterally to the MNTB

501   and SPN is the linear medial superior olive (MSO) (a, b with outline in c). The lateral superior

502   olive (LSO) (outline in c) can be seen lateral to the MSO and contains a marginal (lso-m) and

503   core (lso-c) regions (outlines in a, c). The boundary of the LSO shown in panel c is tentative and

504   derive from alignment of neuronal somata. Micrographs are taken at 2x (a) and 10x (b). Section

505   coordinates in panel (c) are for all sections. Scale bars denote 1mm in a and 200µm in b, c.

506   Abbreviations: lso – lateral superior olive, mntb – medial nucleus of the trapezoid body, mso –

507   medial superior olive, spn- superior paraolivary nucleus, tb – trapezoid body.

508

Figure 1

Characteristic ABR recording from the dat-tailed dunnart (tone burst indicated with black bar below the graph, 47.5kHz, 5ms duration, 52dB SPL).

Grey line represents the background noise from the recording equipment. Main peaks of ABR indicated by roman numerals and accompanied by abbreviated corresponding auditory nuclei. AN – auditory nerve, CV- cochlear nuclei, SOC – superior olivary nuclei, LL – lateral lemniscus, IC- inferior colliculus.
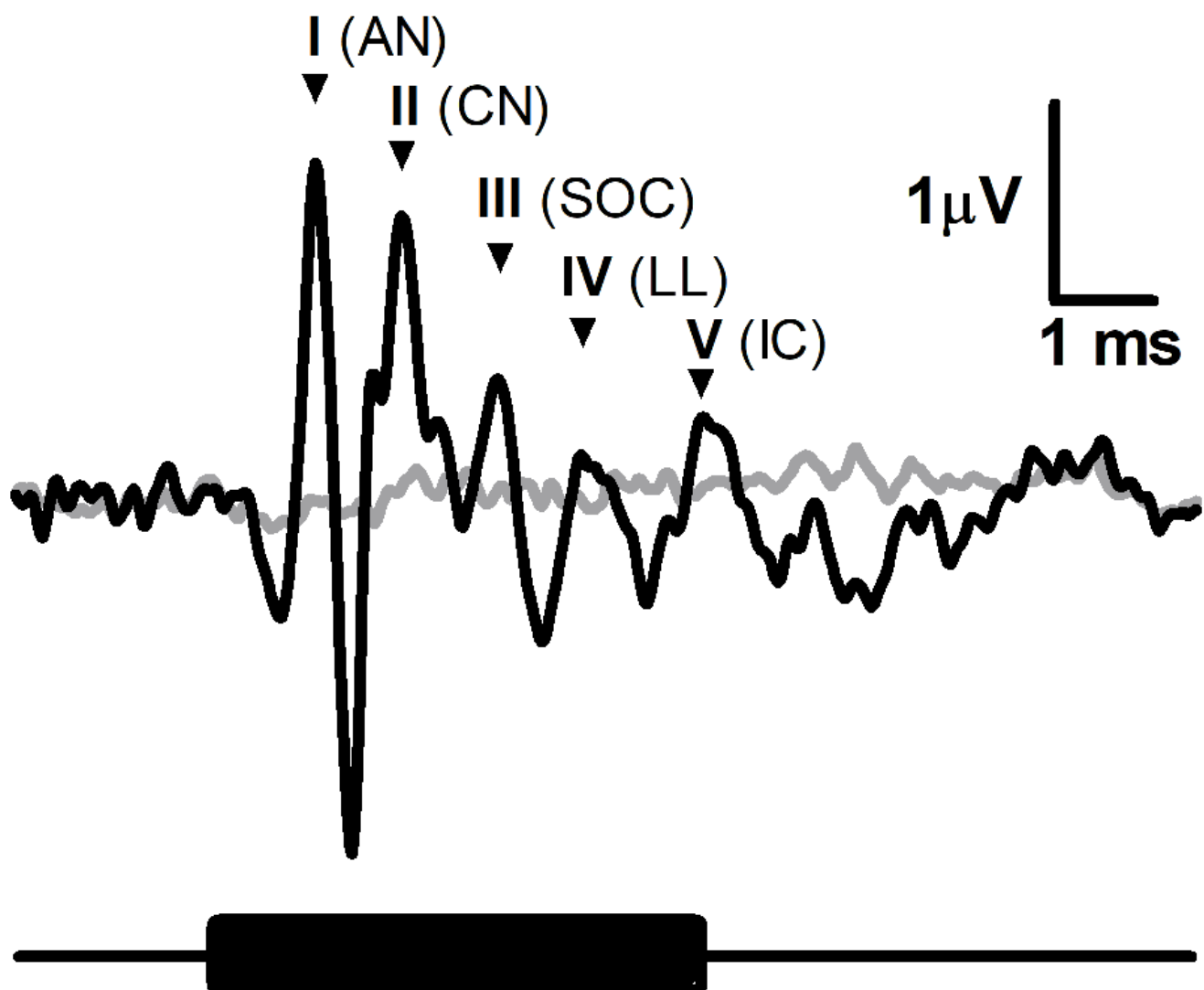
Figure 2

ABR thresholds in fat-tailed dunnart.

(a): ABR recordings at 6 different intensities (42, 32, 22, 12, 7 and 2 dB SPL indicated right of waveforms) in response to a 47.5 kHz tone burst. Waveform corresponding to ABR threshold (disappearance of peaks I and V – shown by asterisks at top) is shown in thick black line. Black bar underneath waveforms indicates duration of tone burst. (b): Audiogram showing ABR thresholds at different frequencies. Individual animal thresholds are shown in grey with numbers in brackets above each point indicate number of animals per data point. Due to several animals with the same thresholds, the number of individual response points, may not appear to correspond with the number of animal in parenthesis (c): Input-output function of the peak I amplitude at 4, 24 and 47.5 kHz. (d) Input-output function of the latency of peak I at 4, 24 and 47.5 kHz. Each data point shows mean ± SEM. N.B. in panel (c) and (d) some of the points at very low sound intensity are the values derived from 1 or 2 animals.
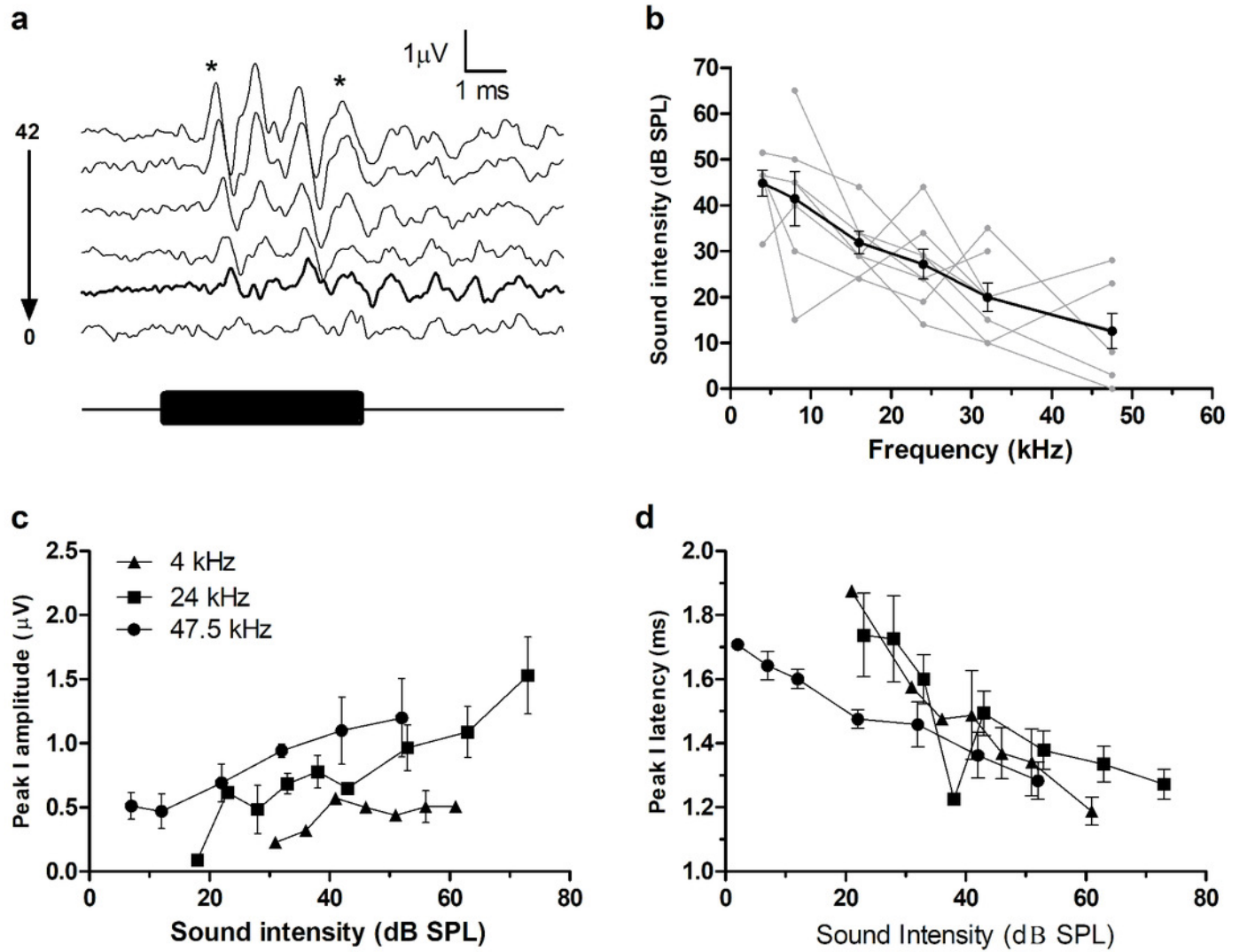
Figure 3

Overview of the fat-tailed dunnart auditory brainstem.

Nissl staining of transverse sections reveals prominent auditory nerve root nucleus and cochlear nuclei. Images are organised caudal to rostral. The dorsal cochlear nucleus resides medio-dorsal to the restiform body in the caudal regions (shown in a, with high power image in b). (c and d): More rostrally the ventral cochlear nucleus shows prominently as well. (d), (e), and (f): further rostral the trilaminar arrangement of the dorsal cochlear nucleus is clearly visible (f) as well as the cochlear nerve root nucleus (g). At more rostral level (h) the ventral cochlear nucleus shows a separation between posteroventral and anteroventral cochlear nucleus. Scale bars are 500µm in a, c, e, h and 200µm in b,d and f,g. Distance between panel a and c: 240µm, between c and e 90µm, and between e and h 210µm. Section coordinates in panel (h) are for all sections. Abbreviations: cnr – cochlear nerve root, cb – cerebellum, dcn – dorsal cochlear nucleus, fn – facial nucleus, rb – restiform body, avcn – anteroventral cochlear nucleus, pvcn- posteroventral cochlear nucleus, in panel f: I – molecular later II – fusiform layer III – polymorphic layer

a

cb

rb

b

dcn

rb

c

scc dcn

pvcn

d

scc dcn

pvcn

e

dcn

pvcn

cnr

fn

f

scc I

II

III

pvcn

g

cnr

h

avcn

D

L
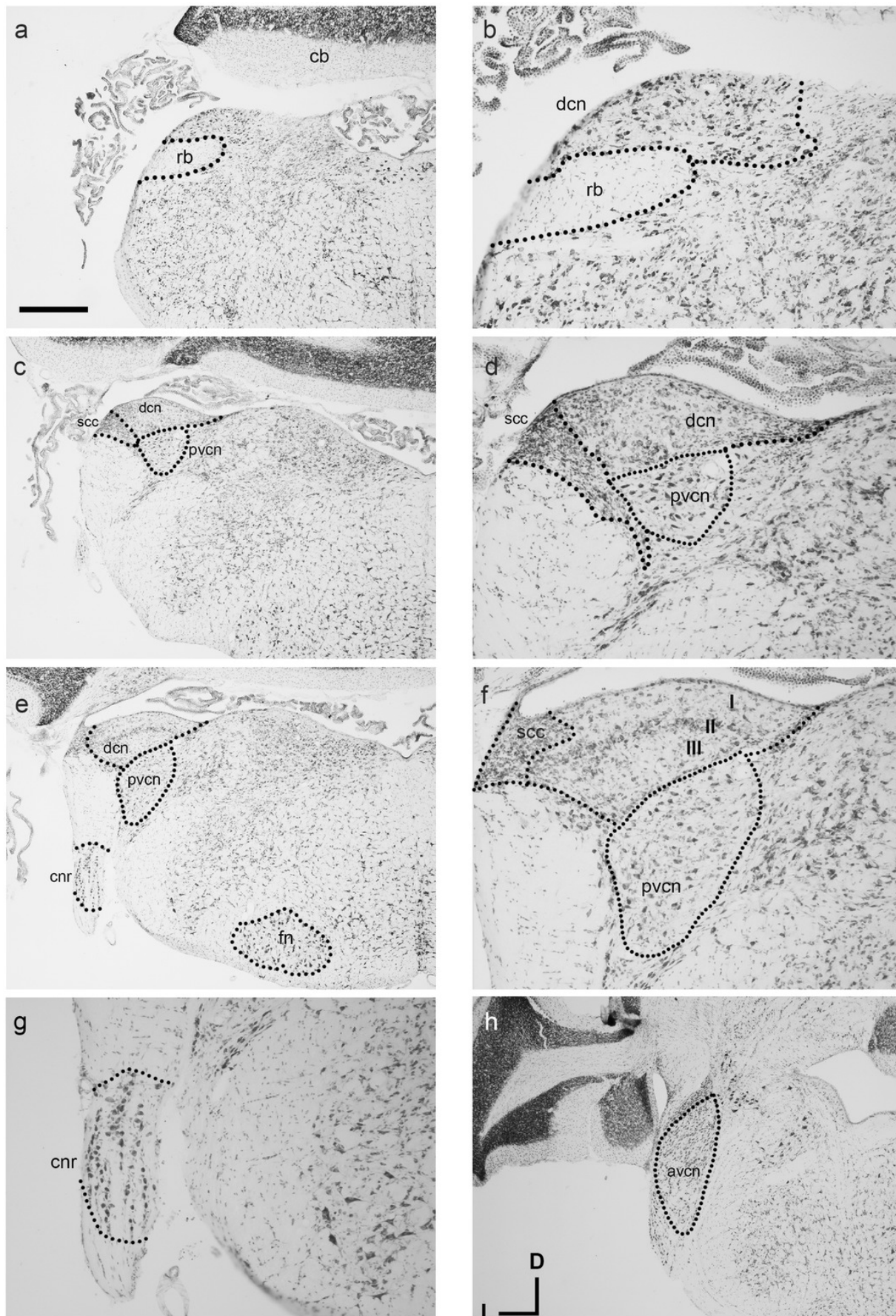
Figure 4

The superior olivary complex (SOC) nuclei in the fat-tailed dunnart.

The four main nuclei evident include the medial nucleus of the trapezoid body (MNTB) (a and b) residing within the fibres of the trapezoid body (tb marked in a). The superior paraolivary nucleus (SPN) is located dorsomedial to the MNTB. Located laterally to the MNTB and SPN is the linear medial superior olive (MSO) (a, b with outline in c). The lateral superior olive (LSO) (outline in c) can be seen lateral to the MSO and contains a marginal (lso-m) and core (lso-c) regions (outlines in a, c). The boundary of the LSO shown in panel c is tentative and derive from alignment of neuronal somata. Micrographs are taken at 2x (a) and 10x (b). Section coordinates in panel (c) are for all sections. Scale bars denote 1mm in a and 200mm in b, c. Abbreviations: lso – lateral superior olive, mntb – medial nucleus of the trapezoid body, mso – medial superior olive, spn- superior paraolivary nucleus, tb – trapezoid body.

a

lso (c)

lso (m)

mso

spn

mntb

b

mso   spn

mntb

c

lso-(c)

lso (m)

mso

spn

D

L